JOURNAL OF VIROLOGY, Apr. 2008, p. 3220–3235 Vol. 82, No. 7
0022-538X/08/$08.00+0 doi:10.1128/JVI.02377-07

Structural Basis for Potent Cross-Neutralizing Human Monoclonal Antibody Protection against Lethal Human and Zoonotic Severe Acute Respiratory Syndrome Coronavirus Challenge▽

Barry Rockx,[1]† Davide Corti,[2]† Eric Donaldson,[3] Timothy Sheahan,[3] Konrad Stadler,[4] Antonio Lanzavecchia,[2] and Ralph Baric[1,3]*

Department of Epidemiology[1] and Department of Microbiology and Immunology,[3] University of North Carolina, Chapel Hill, North Carolina; Institute for Research in Biomedicine, Bellinzona, Switzerland[2]; and Novartis Vaccines, Via Fiorentina 1, 53100 Siena, Italy[4]

Received 2 November 2007/Accepted 8 January 2008

Severe acute respiratory syndrome coronavirus (SARS-CoV) emerged in 2002, and detailed phylogenetic and epidemiological analyses have suggested that it originated from animals. The spike (S) glycoprotein has been identified as a major component of protective immunity, and 23 different amino acid changes were noted during the expanding epidemic. Using a panel of SARS-CoV recombinants bearing the S glycoproteins from isolates representing the zoonotic and human early, middle, and late phases of the epidemic, we identified 23 monoclonal antibodies (MAbs) with neutralizing activity against one or multiple SARS-CoV spike variants and determined the presence of at least six distinct neutralizing profiles in the SARS-CoV S glycoprotein. Four of these MAbs showed cross-neutralizing activity against all human and zoonotic S variants in vitro, and at least three of these were mapped in distinct epitopes using escape mutants, structure analyses, and competition assays. These three MAbs (S109.8, S227.14, and S230.15) were tested for use in passive vaccination studies using lethal SARS-CoV challenge models for young and senescent mice with four different homologous and heterologous SARS-CoV S variants. Both S227.14 and S230.15 completely protected young and old mice from weight loss and virus replication in the lungs for all viruses tested, while S109.8 completely protected mice from weight loss and clinical signs in the presence of viral titers. We conclude that a single human MAb can confer broad protection against lethal challenge with multiple zoonotic and human SARS-CoV isolates, and we identify a robust cocktail formulation that targets distinct epitopes and minimizes the likely generation of escape mutants.

In 2002 to 2003, a novel coronavirus (CoV) caused an outbreak of severe acute respiratory syndrome (SARS), which infected more than 8,000 people and was associated with a ~10% fatality rate (5, 19). In addition, several laboratory-acquired cases of SARS-CoV infection including community spread were reported in 2003 and 2004, highlighting a need for therapeutics (25, 31). Old age (>60 years) was significantly associated with increased SARS-related deaths due to rapidly progressive respiratory compromise (acute respiratory distress syndrome) (5, 26, 40).

SARS-CoV is a zoonotic virus most likely originating from Chinese horseshoe bats, amplified in palm civets and raccoon dogs in the live-animal markets, and subsequently transmitted to human populations (16). The 2003-2004 epidemic has been divided into zoonotic, early, middle, and late phases based on molecular epidemiological studies (6). Comparative analysis of the SARS-CoV genomes from both human and zoonotic isolates throughout the different phases of the epidemic showed a high rate of evolution in the viral attachment protein, the spike (S) glycoprotein, with 23 amino acid changes evolving over the course of the epidemic (37).

Several studies have shown that the SARS-CoV S glycoprotein binds to the receptor angiotensin 1-converting enzyme 2 (ACE2), mediating viral entry (22, 52). A total of 18 amino acids (aa) in ACE2 that are in contact with 14 residues in the receptor binding domain (RBD) of SARS-CoV have been identified (21). Two of these amino acids, aa 479 and 487, have been shown to be critical in the binding of the RBD to human ACE2 and to be linked to cross-species transmission to humans during the epidemic. Not surprisingly, the S glycoprotein has also been identified as a major component of protective immunity and is highly immunogenic, containing at least three domains that are targeted by neutralizing antibodies (10, 13, 20). The exact number of neutralizing epitopes is unknown, as is the effect on neutralization of the sequence variation in these regions between the different S glycoproteins isolated during the SARS-CoV epidemic.

Both human and murine monoclonal antibodies (MAbs) have been developed against three late-phase SARS-CoV strains, strains Urbani, Tor-2, and HKU-39849, and in vitro neutralizing activity has been described (46–48). The recent development of a method to isolate a large number of MAbs from SARS patients provides the reagents needed to characterize the homologous and heterologous neutralizing responses after natural SARS-CoV infection (47). Although

* Corresponding author. Mailing address: Department of Epidemiology, 2107 McGavran-Greenberg, CB#7435, University of North Carolina, Chapel Hill, NC 27699-7435. Phone: (919) 966-3895. Fax: (919) 966-0584. E-mail: rbaric@email.unc.edu.

† B.R. and D.C. contributed equally to this work.

▽ Published ahead of print on 16 January 2008.

studies using pseudotyped lentiviruses and recombinant SARS-CoV RBD protein have shown some cross-neutralizing or cross-reactive activity (12, 24, 43, 56, 57), the neutralizing activities of these MAbs have not been tested against actual heterologous SARS-CoV strains from the middle, early, or zoonotic phase of the epidemic or in lethal models of disease. This is potentially problematic, since the absence of human cases over the past 2 years suggests that future epidemics will likely result from zoonotic transmission. Consequently, antibodies that provide robust cross-neutralization activity are essential to interrupt zoonotic transmission and contain future epidemics (3, 36).

Passive immunization studies on mice, ferrets, and hamsters with select MAbs have demonstrated that some neutralizing antibodies can successfully prevent or limit infection (35, 43, 45, 47). While prophylactic treatment can result in complete protection of rodents from SARS-CoV infection, postinfection treatment is usually less robust but significantly reduces viral titers in the lung (35). To date, all studies have been performed with young animals, allowing for virus replication in the absence of detectable clinical symptoms and disease (37, 42), so it is not clear whether select antibodies will prevent clinical disease or provide measurable levels of protection against homologous or heterologous lethal challenge, especially in more vulnerable senescent populations.

Passive protection of senescent populations has also been poorly studied, yet aged populations are most vulnerable to severe and fatal SARS-CoV infections (5, 26, 40). In the aged BALB/c mouse model, passive transfer of hyperimmune SARS-CoV antiserum from mice prevented infection with the homologous late-phase strain Urbani (51). The use of human MAbs for prevention or treatment of lethal heterologous SARS-CoV infection in aged populations, however, has not been studied in detail. In addition, the recently reported vaccine failure in aged populations makes passive immunization an attractive alternative (8).

We recently developed several lethal SARS-CoV challenge models with BALB/c mice that recapitulated the age-related clinical signs, weight loss exceeding 20% as well as severe lung pathology, by using recombinant SARS-CoV bearing the S glycoprotein of early human and zoonotic strains (37). A second pathogenic model for young mice was also developed by serial passage of the Urbani isolate in BALB/c mice, resulting in MA15, which replicates to high titers in the lung and causes clinical disease, weight loss exceeding 20%, and severe alveolitis (33). In the present study, we used a panel of isogenic SARS-CoVs bearing human and zoonotic S glycoproteins to categorize the human MAbs into six distinct neutralization profiles. Moreover, we identify four neutralizing antibodies that neutralize all zoonotic and human strains tested, and we demonstrate that three of these MAbs engage unique epitopes in the S glycoprotein, providing for the development of a broad-spectrum therapeutic that protects young and senescent mice from lethal homologous and heterologous challenge. A cocktail of these antibodies would likely provide robust protection from lethal SARS-CoV infection in humans.

MATERIALS AND METHODS

Viruses and cells. The generation and characterization of the recombinant infectious clones (ic) of Urbani—icCUHK-W1, icGZ02, icHC/SZ/61/03, icA031G, and icMA15—have been described previously (33, 37). Briefly, the Urbani spike gene in icUrbani was replaced by the various spike genes of CUHK-W1, GZ02, HC/SZ/61/03, and A031G. All recombinant icSARS-CoV strains were propagated on Vero E6 cells in Eagle's minimal essential medium (Invitrogen, Carlsbad, CA) supplemented with 10% fetal calf serum (HyClone, Logan, UT), kanamycin (0.25 μg/ml), and gentamicin (0.05 μg/ml) at 37°C in a humidified CO_2 incubator. All work was performed in a biological safety cabinet in a biosafety level 3 laboratory containing redundant exhaust fans. Personnel were equipped with powered air-purifying respirators with high-efficiency particulate air and organic vapor filters (3M, St. Paul, MN), wore Tyvek suits (DuPont, Research Triangle Park, NC), and were double gloved.

Human MAbs. Human MAbs against SARS-CoV were generated as described previously (47). The MAbs were initially screened for their capacity to bind to SARS-CoV S-expressing cells and were subsequently tested for their ability to neutralize the Frankfurt isolate of SARS-CoV (GenBank accession number AY310120). A panel of 23 SARS-CoV S-specific MAbs and a control MAb (D2.2) specific for diphtheria toxin were used for further study.

Neutralization assay. Neutralizing titers were determined by either a microneutralization assay or a plaque reduction neutralization titer assay (37). For the microneutralization assay, MAbs were serially diluted twofold and incubated with 100 PFU of the different icSARS-CoV strains for 1 h at 37°C. The virus and antibodies were then added to a 96-well plate with 5×10^3 Vero E6 cells/well and 5 wells per antibody dilution. Wells were checked for cytopathic effect (CPE) at 4 to 5 days postinfection, and the 50% neutralization titer was determined as the MAb concentration at which at least 50% of wells showed no CPE. For the plaque reduction neutralization titer assay, MAbs were serially diluted twofold and incubated with 100 PFU of the different icSARS-CoV strains for 1 h at 37°C. The virus and antibodies were then added to a 6-well plate with 5×10^5 Vero E6 cells/well in duplicate. After a 1-h incubation at 37°C, cells were overlaid with 3 ml of 0.8% agarose in medium. Plates were incubated for 2 days at 37°C and then stained with neutral red for 3 h, and plaques were counted. The percentage of neutralization was calculated as [1 − (number of plaques with antibody/number of plaques without antibody)] × 100. All assays were performed in duplicate. Importantly, a good correlation has been noted between the two assays (data not shown).

Inhibition of binding of SARS-CoV spike glycoprotein to ACE2. Serial dilutions of MAbs in phosphate-buffered saline (PBS)–1% fetal calf serum were incubated for 20 min at 4°C with 5 μg/ml SARS-CoV S glycoprotein (S1 domain, aa 19 to 713 of the WH20 isolate [99.8% amino acid homology with Urbani]; accession number AY772062) fused to the Fc region of human immunoglobulin (Ig) (Aalto Bio Reagents, Dublin, Ireland). The mixture was added to a single-cell suspension of 4×10^4 ACE2-transfected DBT cells that had been sorted for stable and relatively uniform levels of ACE2 expression. After 20 min, the cells were washed and stained with phycoerythrin-conjugated $F(ab')_2$ fragments of a goat anti-human Fcγ specific antibody (Jackson ImmunoResearch Laboratories). The percentage of binding inhibition was calculated as [1 − (% positive events for the sample/B_{max})] × 100, where maximum binding (B_{max}) is represented by the average of six wells. The concentration of the antibody needed to achieve 50% binding inhibition was calculated with GraphPad Prism software using nonlinear regression fitting with a variable slope.

Detection of human MAbs. The reactivities of MAbs with native or denatured Urbani S recombinant protein were determined by enzyme-linked immunosorbent assays (ELISA). Briefly, 96-well plates were coated with 1 μg/ml of recombinant Urbani S glycoprotein (NR-686; NIH Biodefense and Emerging Infections Research Resources Repository, NIAID, NIH). Wells were washed and blocked with 5% nonfat milk for 1 h at 37°C and were then incubated with serially diluted MAbs for 1.5 h at 37°C. Bound MAbs were detected by incubating alkaline phosphatase-conjugated goat anti-human IgG (A-1543; Sigma) for 1 h at 37°C and were developed by 1 mg/ml *p*-nitrophenylphosphate substrate in 0.1 M glycine buffer (pH 10.4) for 30 min at room temperature. The optical density (OD) values were measured at a wavelength of 405 nm in an ELISA reader (Bio-Rad model 680).

Competition for binding to SARS-CoV S glycoprotein. MAbs were purified on protein G columns (GE Healthcare) and biotinylated using the EZ-Link NHS-PEO solid-phase biotinylation kit (Pierce). An ELISA was used as described above to measure the competition between unlabeled and biotinylated MAbs for binding to immobilized SARS-CoV S glycoprotein. Unlabeled competitor MAbs were added at 5 μg/ml. After 1 h, biotinylated MAbs were added at a limiting concentration (0.1 μg/ml) that was chosen to give a net OD in the linear part of the titration curve, allowing the inhibitory effects of the unlabeled MAb to be quantitated. After incubation for 1 h, the plates were washed, and the amount of biotinylated MAb bound was detected using alkaline phosphatase-labeled streptavidin (Jackson ImmunoResearch). The percentage of inhibition was cal-

TABLE 1. Experimental design of passive immunization studies on mice

Expt	Amt of MAb (μg)	MAb(s)	Day(s) of vaccination	Challenge virus(es)	Age of mice
1	25	D2.2, S109.8, S227.14, S230.15	−1	icUrbani, icGZ02, icHC/SZ/61/03	12 mo
2	250	D2.2, S109.8, S227.14, S230.15	−1	icUrbani, icGZ02, icHC/SZ/61/03	12 mo
3	250	S109.8 + S227.14 + S230.15 (cocktail)	−1	icHC/SZ/61/03	12 mo
4	250	S230.15	−1	icHC/SZ/61/03	10 wk
5	25	D2.2, S109.8, S227.14, S230.15	−1	icMA15	10 wk
6	250	S230.15	−1, 0, 1, 2, 3	GZ02	12 mo

culated with the means of triplicate tests as $(1 - [(OD_{sample} - OD_{negative\ control})/(OD_{positive\ control} - OD_{negative\ control})]) \times 100$.

Escape mutant analysis. Thirty micrograms of a neutralizing antibody was incubated with 1×10^6 PFU of icGZ02 for 30 min at room temperature in a 0.25-ml volume and was then inoculated onto six-well dishes containing 1×10^6 cells. After a 1-h incubation, the inoculating virus was removed, and 1 ml of medium containing 30 μg of the appropriate antibody was added to the culture wells. The development of CPE was monitored over 72 h, and progeny viruses were harvested at ~25 to 50% CPE. Antibody treatment was repeated two additional times, and more-rapid CPE was noted with each passage. Passage 3 viruses were plaque purified in the presence of a MAb, and neutralization-resistant viruses were isolated and designated GZ02-230 and GZ02-109-1 and -2. The S genes of individual plaques were sequenced as previously described (37). The neutralization titers for wild-type and MAb-resistant viruses were determined as described above.

Structural analyses. The crystal structure coordinates of the SARS-CoV RBD interacting with the human ACE2 receptor (PDB code 2AJF) (21) were used as a template to generate each set of mutations using the Rosetta Design Web server (http://rosettadesign.med.unc.edu/). In each case, the SARS-CoV RBD structure was analyzed by using the molecular modeling tool MacPyMol (DeLano Scientific) to determine which amino acid residues were proximal to the amino acid being targeted for replacement. Briefly, each amino acid to be altered was highlighted, and all other amino acid residues within an interaction distance of 5 Å were identified. Using the Rosetta Design website, the amino acid replacements were incorporated, and all amino acid residues within the 5-Å interaction distance were relaxed to allow the program to repack the side chains to an optimal energetic state. This process was repeated with each mutation and series of mutations. Ten models were generated for each set of mutations, and the best model was selected based on the lowest energy score and was further evaluated using Mac Pymol. In all cases, the lowest energy scores were identical for several of the predicted models, suggesting an optimal folding energy of the chosen model.

Passive immunization. Female BALB/cAnNHsd mice (age, 10 weeks or 12 months; Harlan, Indianapolis, IN) were anesthetized with a ketamine (1.3 mg/mouse)–xylazine (0.38 mg/mouse) mixture administered intraperitoneally in a 50-μl volume. Each mouse was intranasally inoculated with 10^6 PFU (icUrbani, icGZ02, or icHC/SZ/61/03) or 10^5 PFU (icMA15) of icSARS-CoV in a 50-μl volume.

In experiments 1 and 2 (Table 1), 12-month-old mice were injected intraperitoneally with 25 or 250 μg of various human MAbs (D2.2, S109.8, S227.14, or S230.15) in a 400-μl volume at 1 day prior to intranasal inoculation with 10^6 PFU of the different icSARS-CoV strains ($n = 3$ per MAb per virus per time point). In experiment 3 (Table 1), 12-month-old mice were injected with a cocktail of S109.8, S227.14, and S230.15 (containing 83 μg of each MAb) with a total concentration of 250 μg MAb in 400 μl at 1 day prior to inoculation with 10^6 PFU icHC/SZ/61/03 ($n = 3$ per time point). In experiment 4 (Table 1), 10-week-old mice were injected with 250 μg of S230.15 at 1 day prior to inoculation with 10^6 PFU of icHC/SZ/61/03 ($n = 4$). In experiment 5 (Table 1), 10-week-old mice were injected with 25 μg of D2.2, S109.8, S227.14, or S230.15 at 1 day prior to inoculation with 10^5 PFU of icMA15 ($n = 3$ per MAb per time point). In experiment 6 (Table 1), 12-month-old mice were injected with 250 μg of S230.15 at −1, 0, 1, 2, or 3 days after inoculation with 10^6 PFU icGZ02 ($n = 5$ per treatment per time point). All animals were weighed daily, and at 2, 4, or 5 days postinfection, serum and lung samples were removed and frozen at −70°C for later determination of viral titers by plaque assays. Lung tissue was also removed for histological examination on day 4 or 5 depending on whether animals had to be euthanized due to >20% weight loss.

All mice were housed under sterile conditions in individually ventilated Sealsafe cages using the SlimLine system (Tecniplast, Exton, PA). Experimental protocols were reviewed and approved by the Institutional Animal Care and Use Committee at the University of North Carolina, Chapel Hill.

Virus titers in lung samples. Tissue samples were weighed and homogenized in 5 equivalent volumes of PBS to generate a 20% solution. The solution was centrifuged at 13,000 rpm under aerosol containment in a tabletop centrifuge for 5 min; the clarified supernatant was serially diluted in PBS; and 200-μl volumes of the dilutions were placed on monolayers of Vero cells in 6-well plates. Following a 1-h incubation at 37°C, cells were overlaid with a medium containing 0.8% agarose. Two days later, plates were stained with neutral red, and plaques were counted.

Histology. All tissues were fixed in 4% paraformaldehyde in PBS (pH 7.4) prior to being submitted to the Histopathology Core Facility (University of Norrth Carolina, Chapel Hill) for paraffin embedding, sectioning at a 5-μm thickness, and hematoxylin and eosin staining. Lung pathology was evaluated in a blinded manner.

RESULTS

Identification of cross-neutralizing MAbs. A panel of 23 human MAbs was tested for neutralizing activity against one or multiple icSARS-CoV bearing spike variants from the late, middle, early, and zoonotic phases of the epidemic. The panel includes a number of new MAbs (S228.11, S222.1, S237.1, S223.4, S225.12, S226.10, S231.19, S232.17, S234.6, S227.14, S230.15, S110.4, and S111.7) that were not described in the initial study (47) and that, except for S110.4 and S111.7, were all isolated at a late time point after infection with SARS-CoV (2 years). All MAbs efficiently neutralized the late-phase icUrbani isolate (Table 2), which was homologous to the strain isolated from the patient used to produce the MAbs (50). Interestingly, in testing of the MAbs against the middle-phase, early-phase, and zoonotic isolates, six distinct neutralization patterns were identified (Table 2). Two unique group I MAbs that specifically neutralized the homologous late-phase isolate, icUrbani, were identified. Two MAbs that neutralized the homologous icUrbani strain about 10-fold more efficiently than the middle-phase isolate, icCUHK-W1, comprise group II. Group III contains five MAbs that were about 50-fold more efficient at neutralizing the icUrbani reference strain than the group I antibodies. These antibodies were extremely efficient at neutralizing the human late-, middle-, and early-phase isolates ($n = 5$), but not the zoonotic isolates, at all concentrations tested (8 ng/ml to 16 μg/ml). Group IV consists of eight MAbs that were extremely efficient at neutralizing the human isolates as well as the palm civet isolate icHC/SZ/61/03. It is likely that two or more neutralizing epitopes exist within this cluster, since some MAbs were equally efficient at neutralizing human and zoonotic isolates (e.g., MAbs 225.12, 226.10, and 234.6) while others required a 10-fold-higher concentration to neutralize the civet isolate (e.g., MAbs 218.9, 231.19, and 232.17). The group V cluster consists of two MAbs that neutralized variable subsets of the human and zoonotic strains, but only at high concentrations. Finally, group VI consists of four MAbs that neutralized all human and zoonotic strains available within our panel of variant SARS-CoV spike variants. Because of the different concentrations of antibody needed to neutralize isolates for each MAb in group VI, we suspected that at least two or three different panspecific neutralizing epitopes likely exist in the SARS-CoV S glycoprotein.

TABLE 2. Characterization of a panel of human MAbs for their capacities to neutralize human and zoonotic SARS-CoV strains and to inhibit the binding of the SARS-CoV S glycoprotein to human ACE2[a]

Group	MAb	50% Neutralization titer (ng/ml)[b] for the indicated virus								Inhibition of SARS-CoV S binding to ACE-2[c]	
		Human			Zoonotic		Neutralization escape variant				
		Late (Urbani)	Middle (CUHK-W1)	Early (GZ02)	Palm civet (HC/SZ/61/03)	Raccoon dog (A031G)	GZ02-109-1	GZ02-109-2	GZ02-230	% Inhibition	IC_{50} (ng/ml)
I	S132	1,984	–	–	–	–	NT	NT	NT	60	2,570
	S228.11	196	–	–	–	–	NT	NT	NT	97	598
II	S111.7	154	1,232	–	–	–	NT	NT	NT	96	1,208
	S224.17	194	1,552	–	–	–	NT	NT	NT	98	297
III	S3.1	45	180	720	–	–	NT	NT	NT	96	868
	S127.6	65	259	518	–	–	NT	NT	NT	97	876
	S217.4	30	59	118	–	–	NT	NT	NT	99	114
	S222.1	51	202	808	–	–	NT	NT	NT	98	98
	S237.1	8	67	34	–	–	NT	NT	NT	97	66
IV	S110.4	81	322	644	1,288	–	NT	NT	NT	99	476
	S218.9	31	123	246	1,968	–	NT	NT	NT	101	280
	S223.4	20	79	158	316	–	NT	NT	NT	99	112
	S225.12	9	18	72	72	–	NT	NT	NT	99	68
	S226.10	23	90	360	180	–	NT	NT	NT	99	92
	S231.19	18	71	141	2,256	–	NT	NT	NT	99	120
	S232.17	90	180	360	2,880	–	NT	NT	NT	100	95
	S234.6	64	2,032	254	254	–	NT	NT	NT	100	142
V	S124.5	1,400	5,600	–	1,120	5,600	NT	NT	NT	56	4,700
	S219.2	248	992	–	–	496	NT	NT	NT	44	>3,000
VI	S109.8	424	848	3,392	424	53	–	–	3,300	85	525
	S215.17	25	100	200	400	3,200	NT	NT	NT	98	200
	S227.14	19	77	153	306	77	150	150	150	100	126
	S230.15	20	40	160	160	80	155	155	–	99	84

[a] A panel of 23 human mAbs was tested for their capacities to neutralize recombina NT SARS-CoV S glycoprotein variants (Urbani, CUHK-W1, GZ02, HC/SZ/61/03, and A031G) and neutralization escape variants (GZ02-109-1, GZ02-109-2, and GZ02-230). MAbs are ranked in six groups according to their capacities to neutralize different SARS-CoV S glycoprotein variants.

[b] MAb concentration at which 50% of the viruses are neutralized. –, no neutralizing titer detected at 10 μg/ml; NT, not tested.

[c] The percentage of maximal inhibition by each MAb of SARS-CoV S glycoprotein binding to human ACE2 expressed by murine DBT cells is shown, along with the concentration at which 50% of the binding is blocked (IC_{50}).

Identification of MAbs that inhibit the binding of the SARS-CoV S glycoprotein to ACE2. To identify the MAbs that directly inhibit the binding of SARS-CoV to its cellular receptor, ACE2, as a mechanism of neutralization, we assessed the capacity of the MAb panel described above to inhibit the binding of the SARS-CoV S1 domain to human ACE2 expressed on the surfaces of transfected murine DBT cells. The antibody activity is expressed as the concentration that blocks 50% of spike binding to ACE2 and as maximum-inhibition values (Table 2). Most of the antibodies completely inhibited binding, although with different potencies (Table 2; see, for example, S230.15 and S3.1). Of note, some antibodies only partially inhibited the binding of the spike protein, even when tested at the highest concentrations (Table 2; see, for example, S124.5 and S109.8). Not surprisingly, a significant correlation was observed between neutralization titers and inhibition titers for the binding of the SARS-CoV S glycoprotein to ACE2 (r^2 = 0.344; P = 0.002). However, a few antibodies, such as S3.1 and S127.6, showed a high virus neutralization capacity in spite of a low capacity to interfere with the binding of the spike protein to its receptor (Table 2).

Sequence analysis of virus neutralization. By using a panel of S glycoprotein variants, the amino acid changes associated with loss of neutralization can be identified. To identify possible locations of neutralizing epitopes recognized by these MAbs, the neutralization groups were annotated in accordance with the amino acid sequence variations noted in the different S glycoproteins used in this study (Fig. 1A). Interestingly, group I MAbs S132 and S228.11 uniquely neutralized icUrbani, which differs at positions G77D and I244T in the S1 domain from the resistant middle-phase isolate icCUHK-W1 (Fig. 1A). Although the mechanism is unclear, these two unique residues in icUrbani, either individually or in concert, result in either (i) microvariation within overlapping epitopes, (ii) changes in conformational epitopes, or (iii) mutations that alter the surface topology of a group I epitope. In accordance with these findings, four amino acid differences (Fig. 1A) were observed between the middle-phase icCUHK-W1 and the early-phase icGZ02 S glycoprotein. The fact that group II antibodies efficiently inhibit RBD binding to ACE2 implies that the critical residues are likely those residing within the RBD (G311R and K344R). In contrast, the mutations that

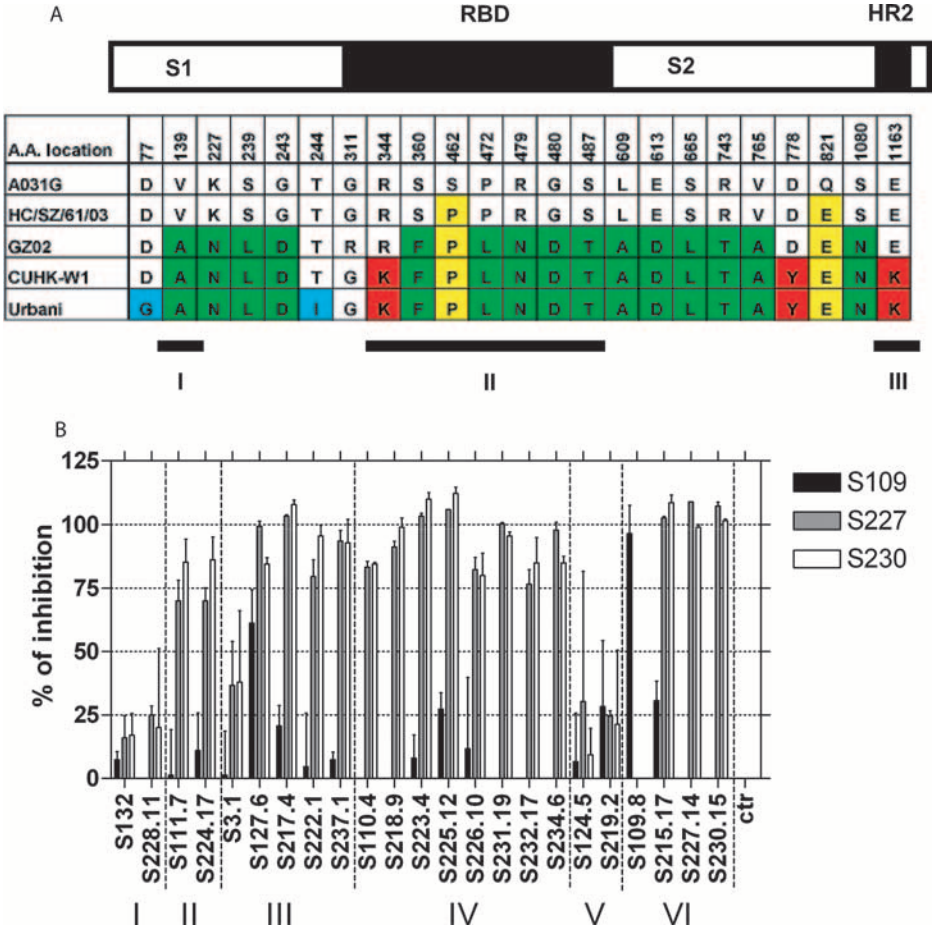

FIG. 1. Mapping of neutralizing epitopes on the SARS-CoV S glycoprotein recognized by human MAbs through sequence analysis and cross-competition studies. (A) Sequence analysis of the amino acid differences in the SARS-CoV S glycoproteins of zoonotic and human epidemic isolates and their associations with binding to neutralizing human MAbs. The graphic representation of the SARS-CoV S glycoprotein shows the locations of the variant amino acids in the RBD and heptad repeat 2 (HR2). Three neutralizing domains have previously been identified by using murine MAbs and antisera targeting the S glycoprotein. Domain I is localized in the N terminus of the S1 domain between amino acid residues 130 and 150; however, the mechanism by which these antibodies neutralize infectivity remains unknown (10). Domain II includes the RBD (residues 318 to 510), where antibodies likely block binding to the SARS-CoV receptor ACE2, based on studies describing the crystal structures of two different neutralizing MAbs in complex with the RBD (13, 15, 32). Finally, domain III includes HR2 (residues 1143 to 1157) and is likely neutralized by disturbing the interaction between HR2 and HR1, thereby abolishing fusion activity (20). Amino acids associated with recognition by MAbs are color coded as follows: blue, group I MAbs; red, group II MAbs; green, group III MAbs; yellow, group IV MAbs. MAb groups are shown in Table 2 and defined in the text under "Identification of cross-neutralizing MAbs." (B) Cross-competition of MAbs binding to the SARS-CoV S glycoprotein. Shown are the percentages of inhibition of the binding of 3 biotinylated MAbs (S109.8, S227.14, and S230.15; concentration, 0.1 μg/ml) to the recombinant SARS-CoV S glycoprotein by a panel of 23 unlabeled competing MAbs (at a saturating concentration [5 μg/ml]) belonging to groups I through VI. Error bars, standard deviations from triplicates. ctr, control.

influence the binding and activity of the group III MAbs are the most complex and are influenced by 1 or more of 15 amino acid differences between the early-phase icGZ02 and the zoonotic palm civet icHC/SZ/61/03 isolate. These amino acids are scattered throughout the S1, RBD, and S2 domains (Fig. 1A); however, all group III antibodies efficiently inhibit RBD binding to ACE2, suggesting that the critical residues are those residing within the RBD. The RBD residues include F360, L472, N479, and D480. The neutralization activity of the group IV MAb cluster is heavily influenced by two amino acid differences between the zoonotic strains icHC/SZ/61/03 and icA031G (raccoon dog isolate), located in the RBD (P462S) or in the S2 domain (E821Q) of the S glycoprotein (Fig. 1A). Again, the efficient inhibition of the binding of the RBD to ACE2 suggests that P462S is the critical residue. The recognition domain of the group VI broad-spectrum antibodies must be conserved across the panel, and the location is unclear, although S230.15 has previously been shown by competition ELISA to bind to the RBD in the S glycoprotein (57) and all the group VI MAbs have been shown to interfere with binding to ACE2 expressed on the surface of the cell membrane.

Competition studies for the definition of epitopes recognized by broadly neutralizing MAbs. Our data suggest that the majority of the human MAbs recognize epitopes differentially defined by a few mutations within the RBD. Competition studies were performed to determine the spatial proximity of each of the conformational epitopes recognized by the three most broadly neutralizing MAbs to the other epitopes on the SARS-

CoV S glycoprotein. MAbs S109.8, S227.14, and S230.15 were purified, biotinylated, and tested for their capacities to bind the SARS-CoV spike protein in the presence of other, unlabeled MAbs. In interpreting competition results, it should be taken into account that when two epitopes overlap, or when the areas covered by the arms of the two MAbs overlap, competition should be almost complete. Weak inhibitory or enhancing effects may simply reflect a decrease in affinity owing to steric or allosteric effects (28, 49). The two most potent cross-neutralizing MAbs, S227.14 and S230.15, compete with each other (Fig. 1B) and with all other MAbs except the group I MAbs (S132 and S228.11), the group V MAbs (S124.5 and S219.2), MAb S3.1 (group III), and MAb S109.8 (group VI). MAb S230.15 has a higher affinity than MAb S227.14, as evidenced by the fact that MAb S230.15 competes with MAb S227.14 at a concentration 16-fold lower than that required for MAb S227.14 to compete with S230.15 (46 ng/ml and 738 ng/ml, respectively). MAb S109.8 did not compete with any of the MAbs, although limited inhibition was seen with S127.6 (61% [Fig. 1B]).

Escape mutant analysis of broadly neutralizing MAbs. Isolate icGZ02, which produces lethal infections in aged but not young mice (37), was used to generate antibody neutralization escape mutants by incubating and culturing high titers of virus in the presence of MAbs S109.8, S227.14, and S230.15. After 3 passages, the resulting viruses were plaque purified and tested for neutralization efficacy. The S109.8 escape mutant of icGZ02, in contrast to wild-type icGZ02, was no longer neutralized by S109.8, even at antibody concentrations exceeding 20 μg/ml (Table 2). However, both S227.14 and S230.15 were as effective at neutralizing the S109.8 escape mutant of icGZ02 as they were at neutralizing the wild-type virus.

Similarly, the S230.15 escape mutant was no longer neutralized by S230.15 but was still effectively neutralized by both MAbs S109.8 and S227.14 (Table 2). This finding was particularly interesting because S227.14 had been shown to compete with S230.15 for binding to the RBD; it confirmed that S227.14 and S230.15 recognize overlapping but distinct epitopes. In addition, no escape mutant of MAb S227.14 was isolated in two independent experiments, suggesting that the epitope recognized by MAb S227.14 may be less susceptible to sequence variation, possibly due to the presence of receptor contact residues within its epitope or other steric constraints that reduce the likelihood of escape mutations evolving in this region.

A minimum of five plaques of each escape variant were sequenced in order to identify mutations associated with the antibody escape phenotype. All five plaques of the S230.15 escape mutant contained a single amino acid change at location L443R. Four out of six plaques of the S109.8 escape mutants contained a single amino acid change at T332I, while two plaques contained a single amino acid change in an adjacent residue at position K333N.

Structural modeling of cross-neutralizing epitopes. Recently, the structure of the SARS-CoV RBD complexed with its receptor, ACE2, was resolved, allowing for structural modeling of amino acid changes within the RBD (21). Both mutations observed with the S109.8 escape mutants flank the side of the RBD in a loop that is not in direct contact with the receptor, ACE2 (Fig. 2A). The T332I change results in a protrusion from the surface due to the additional CH_3 group, and the residue becomes strongly hydrophobic. Alternatively, the amino acid change from Lys to Asn at position 333 removes a positive charge. Both mutations clearly affect binding of MAb S109.8. The mechanism of neutralization by S109.8 is unknown but may either involve structural changes to the RBD after binding or provide a steric hindrance that antagonizes receptor binding in some unspecified manner.

Structural analysis of the S230.15 escape mutant showed that subtle remodeling of the receptor binding pocket did not impact the binding of ACE2. The selected arginine mutation residue is likely forced into the binding pocket by surrounding positively charged amino acids. At this site, a binding pocket exists that can accommodate the larger side chain without disrupting interface site interactions (Fig. 2B). However, the presence of arginine at this position likely abolishes the binding of S230.15. These data support the hypothesis that MAb S230.15 neutralizes SARS-CoV by directly blocking the interaction with its receptor, ACE2.

The combined results from the sequence analysis, competition assays, and escape mutant analysis allowed us to identify the amino acids that were associated with the neutralization efficacy of the three different cross-neutralizing MAbs. By mapping the locations of these amino acids onto the crystal structure of the SARS-CoV strain Urbani RBD bound to ACE2, putative locations of the cross-neutralizing epitopes could be identified (Fig. 2C). MAb S230.15 likely recognizes an epitope that includes aa 443, as shown by escape variant analysis, as well as aa 487, as shown by reduced in vitro neutralization of an SZ16 spike variant with a T487S change (57). The epitope recognized by MAb S227.14 partially overlaps with recognized by S230.15 but is not affected by the L443R change identified in the S230.15 escape mutant. Finally, the epitope recognized by S109.8 includes aa 332 and 333, as shown by escape mutant analysis.

Use of human MAbs for prophylaxis in senescent-animal models. Our data strongly support the hypothesis that MAbs S109.8, S227.14, and S230.15 are potent cross-neutralizing human MAbs that recognize the RBD of the SARS-CoV S glycoprotein. S109.8 recognizes a unique epitope distinct from the receptor binding site, while S227.14 and S230.15 recognize partially overlapping epitopes that coincide with the receptor binding site. These broad-spectrum neutralizing MAbs were therefore tested for their abilities to protect against lethal homologous and heterologous SARS-CoV challenges in vivo. Previous studies with a murine model of acute nonlethal challenge indicated that 200 μg of MAb S230.15 was protective against SARS-CoV infection, but MAb prophylaxis had not been studied with aged mice (57). SARS-CoV typically produces severe disease in senescent populations, requiring a prophylactic approach that would protect both young and older populations. We have previously shown that infection of 12-month-old BALB/cBy mice with 10^5 PFU of icGZ02 or icHC/SZ/61/03 resulted in death or >20% weight loss by day 4 or 5 (37), whereas mice infected with 10^5 PFU of icUrbani lost only 10% of their weight. Interestingly, by increasing the challenge titer 10-fold to 10^6 PFU, the typically mild pathogenic phenotype of icUrbani was increased: weight loss for 1-year-old BALB/cAnNHsd mice approached 20% by day 4 or 5 (Fig. 3A, D2.2).

Twelve-month-old BALB/c mice that received 25 μg of

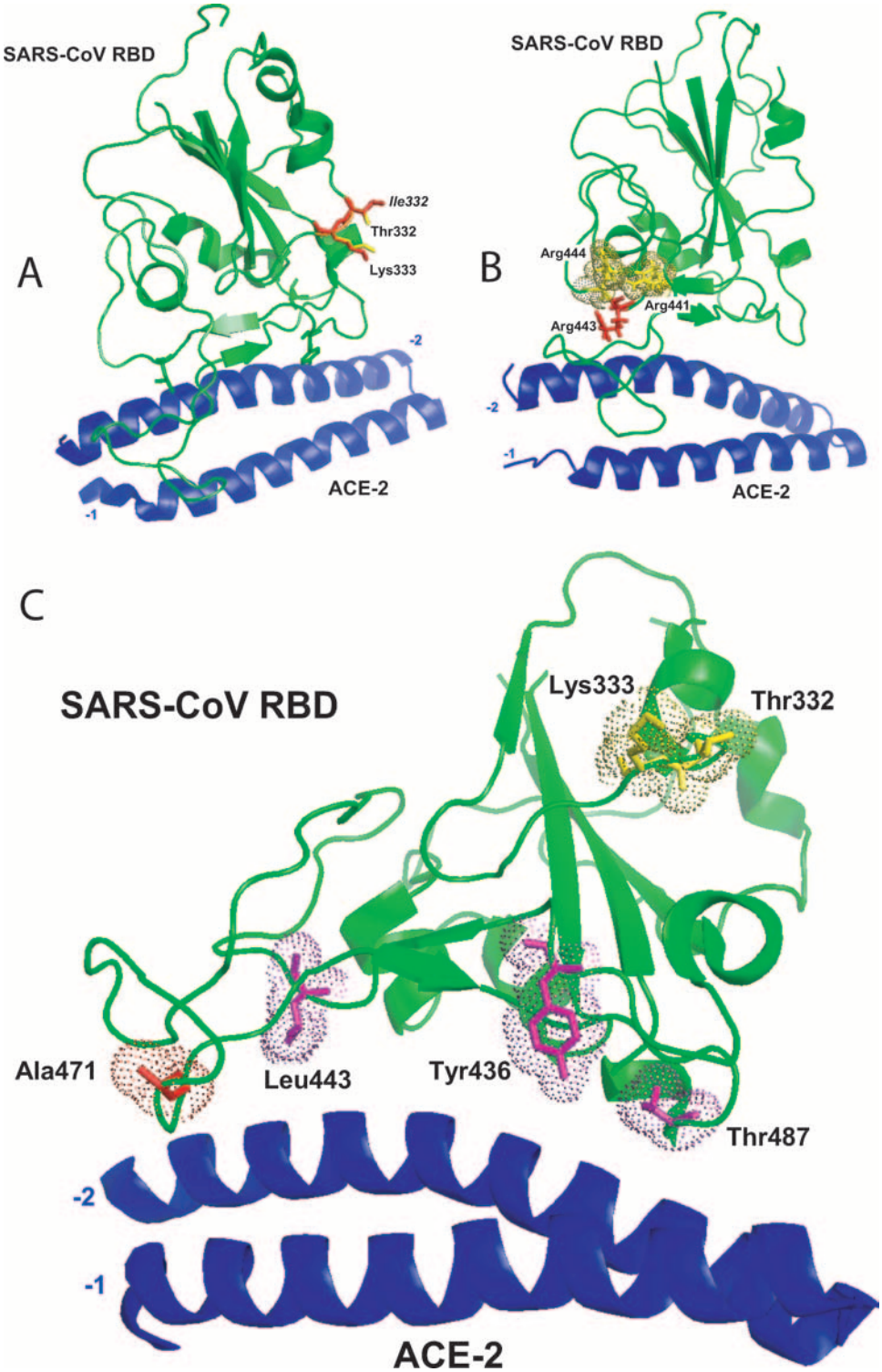

FIG. 2. Locations of neutralization escape variant mutations and effects on the structure of the SARS-CoV RBD. (A and B) The S109.8 escape variant mutations T332I and K333N (A) and the S230.15 escape variant mutation L443R (B) were mapped onto the structure of the SARS-CoV RBD. The changed amino acid residues are shown in red. (C) The locations of all the important amino acid residues associated with the cross neutralizing MAbs are highlighted in the SARS-CoV RBD. Yellow, amino acid residues associated with S109.8; red, amino acid residues associated with S227.14; purple, amino acid residues associated with S230.15.

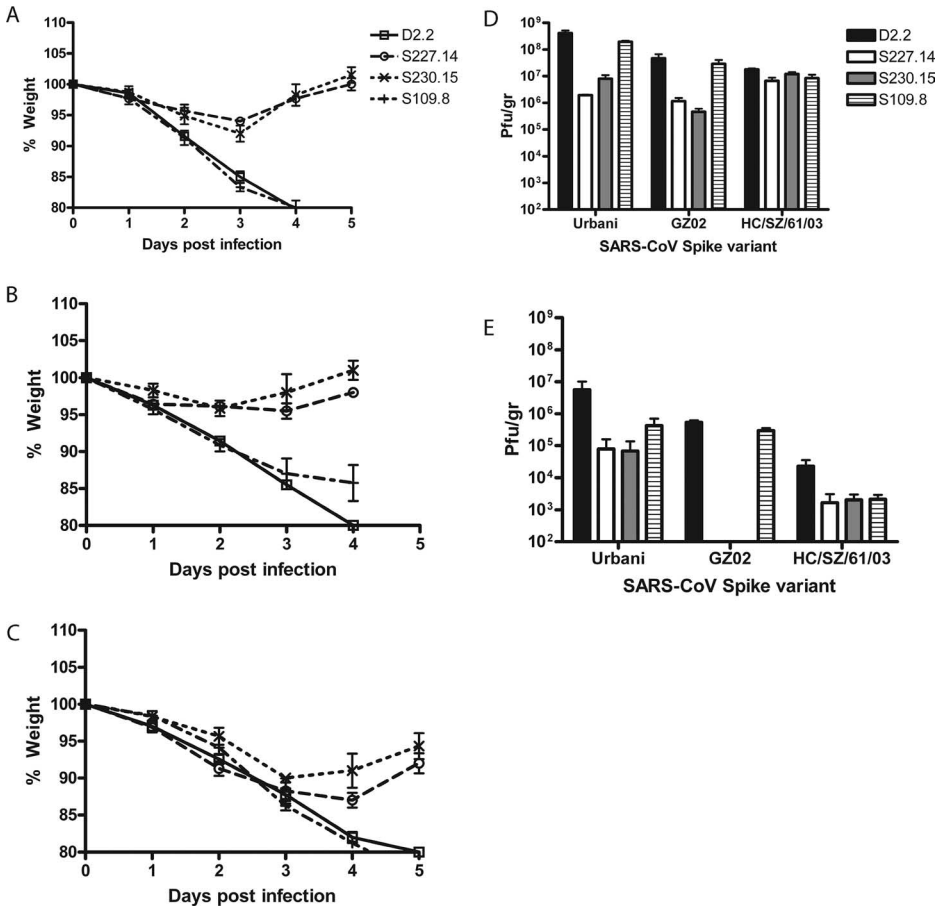

FIG. 3. Prophylactic treatment of lethal SARS-CoV infection in 12-month-old BALB/c mice with 25 μg of cross-neutralizing MAbs. (A to C) Body weights of mice infected with icUrbani (A), icGZ02 (B), or icHC/SZ/61/03 (C) were measured daily after passive transfer of 25 μg of MAb S109.8 (+), S227.14 (○), S230.15 (×), or D2.2 (□). (D and E) Lung tissues were harvested from infected mice on day 2 (D) and day 5 (E) postinfection and were assayed for infectious virus. Error bars, standard deviations ($n = 3$).

MAb S227.14 or S230.15 intraperitoneally 24 h prior to infection were protected against significant weight loss ($P < 0.01$ by the t test) and had reduced viral titers in their lungs on days 2 and 5, approaching reductions of 1.5 to 2 and 2 to 4 log units, respectively, following challenge with icUrbani or icGZ02 (Fig. 3A, B, D, and E). Animals challenged with icHC/SZ/61/03 that had received 25 μg of MAb S227.14 or S230.15 were less efficiently protected but displayed significant reductions in weight loss, which approached 12% of weight by day 4 ($P < 0.01$ by the t test) (Fig. 3C). In addition, all animals receiving MAb S227.14 or S230.15 recovered by day 5. In contrast, animals that received the irrelevant MAb D2.2 or MAb S109.8 were not protected against weight loss after challenge with homologous or heterologous icSARS-CoV; all these animals lost >20% of their weight by day 4 postinfection (Fig. 3C). In addition, virus titers remained high in mice that received S109.8 and were challenged with icUrbani or icGZ02, as well as in all of the BALB/c mice challenged with icHC/SZ/61/03, demonstrating that this antibody was less efficient at protecting animals from lethal infection, especially at low doses (Fig. 3D and E).

We used a very high dose of the challenge inocula to provide the most stringent test for MAb effectiveness, so it was not surprising that a 25-μg MAb dose produced variable results with some MAbs and challenge viruses. To determine whether a high dose of MAb would enhance prophylaxis against clinical disease and death, 12-month-old BALB/c mice were dosed with 250 μg of MAb D2.2, S109.8, S227.14, or S230.15 1 day prior to infection. As expected, animals that received S227.14 or S230.15 were protected against significant weight loss after challenge with icUrbani, icGZ02, or icHC/SZ/61/03 ($P < 0.01$ by the t test) (Fig. 4A, B, and C). Importantly, the 10-fold-increased dose of S109.8 was completely protective; animals did not lose significant weight after challenge with icUrbani or icGZ02 and were partially protected against icHC/SZ/61/03 clinical disease, losing significantly less weight (~10% of weight by day 3; $P < 0.01$ by the t test) than controls relative to icUrbani-challenged animals (Fig. 4A, B, and C). Importantly, animals recovered by day 5 postinfection, demonstrating that the antibody protected against severe clinical disease and death (Fig. 4C). On days 2 and 5 following challenge with icUrbani or icGZ02, no virus could be detected in the lungs of animals that had received S227.14 or S230.15 ($P < 0.01$ by analysis of variance [ANOVA]) (Fig. 4D and E), but interestingly, only >1- and >2-log-unit reductions were observed, respectively, after challenge with icHC/SZ/61/03 ($P < 0.05$ by ANOVA). In the lungs of BALB/c mice that received S109.8, only limited reduc-

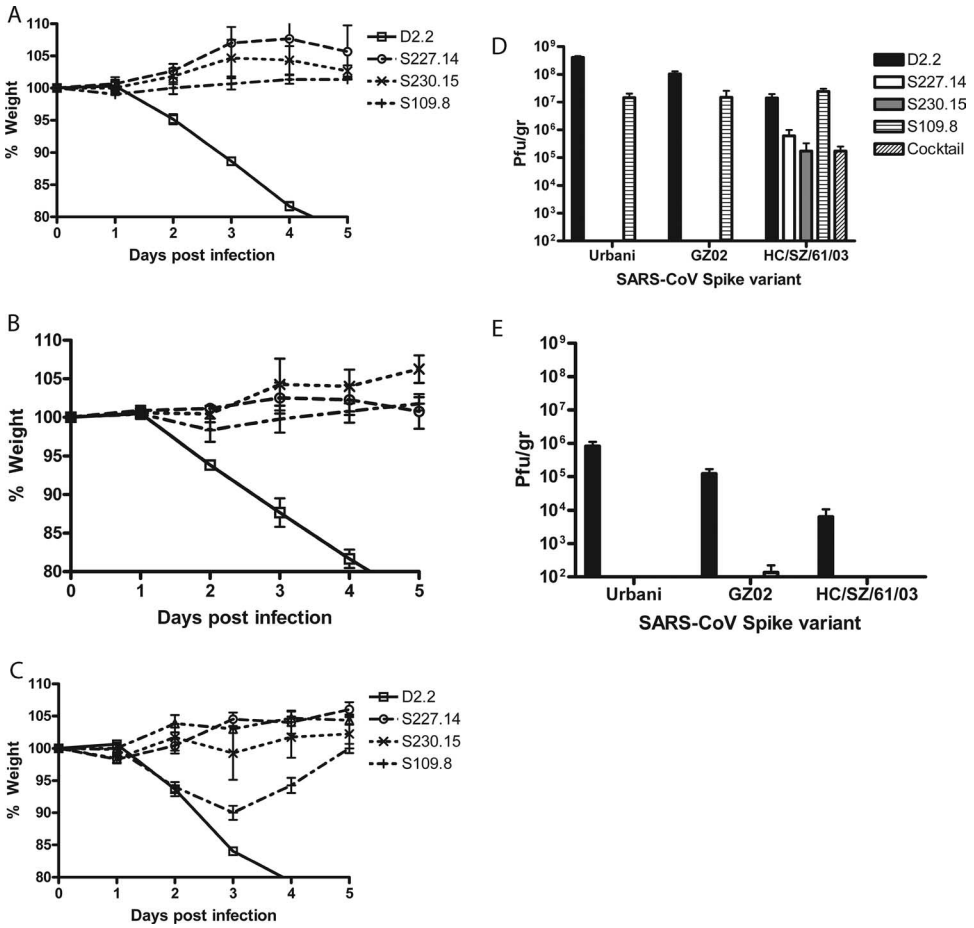

FIG. 4. Prophylactic treatment of lethal SARS-CoV infections in 12-month-old BALB/c mice with 250 μg of cross-neutralizing MAbs. (A to C) Body weights of mice infected with icUrbani (A), icGZ02 (B), or icHC/SZ/61/03 (C) were measured daily after passive transfer of MAbs S109.8 (+), S227.14 (○), S230.15 (×), and D2.2 (□), all at 250 μg/mouse, given alone or as a 1:1:1 cocktail of the three neutralizing MAbs (△). (D and E) Lung tissues were harvested from infected mice on day 2 (D) and day 5 (E) postinfection and were assayed for infectious virus. Error bars, standard deviations ($n = 3$).

tions in viral titers were observed (~1 log unit) on day 2 after challenge with icUrbani or icGZ02 ($P < 0.01$ by ANOVA), and no reduction was observed in icHC/SZ/61/03 titers. However, no viral replication could be detected in the lungs of mice infected with any of the viruses at day 5 postinfection, demonstrating an enhanced rate of clearance over time (Fig. 4E).

Broad-spectrum MAb cocktail. Previous studies have suggested that cocktails of neutralizing antibodies may enhance protection against virus infection (46). Since single-MAb treatment regimens did not protect 12-month-old BALB/c mice against virus replication after challenge with the heterologous strain icHC/SZ/61/03, animals were dosed with a cocktail of equal amounts of MAbs S109.8, S227.14, and S230.15 (83 μg of each MAb) at a final concentration of 250 μg in order to test the hypothesis that multiple MAbs recognizing distinct neutralizing epitopes may increase immunization efficacy. Animals that received the cocktail were completely protected against weight loss following infection with icHC/SZ/61/03 ($P < 0.01$ by the t test) (Fig. 4C). In addition, viral titers in the lungs on day 2 postchallenge (Fig. 4D) were similar to those for animals that received MAb S227.14 or S230.15 alone, but about 2 log units lower than those for animals that received MAb S109.8 alone. As with mice treated with a single MAb, no virus could be detected at 5 days postinfection (Fig. 4E).

Protection of young mice from lethal challenge. MAb S230.15 has recently been shown to protect young mice against replication of recombinant SARS-CoV bearing another palm civet S glycoprotein (SZ16) (37). Surprisingly, the same MAb did not completely protect 12-month-old BALB/c mice against lethal challenge with another civet virus variant, icHC/SZ/61/03. To determine whether the failure of the passive immunization against icHC/SZ/61/03 was specific for aged mice, an identical passive immunization experiment was performed on 10-week-old BALB/c mice. As shown previously for 8-week-old mice (37), young mice challenged with icHC/SZ/61/03 did not lose weight or display other clinical disease symptoms (data not shown), and virus titers in young and old mice were comparable. Interestingly, only one out of three mice that received a 250-μg dose of S230.15 had detectable viral titers (7×10^6 PFU/g), demonstrating enhanced functional activity in younger animals. In control animals, icHC/SZ/61/03 replicates to equivalent titers at day 2 postinfection, suggesting that passive antibody transfer may be less efficient at protecting the lungs of immunosenescent populations.

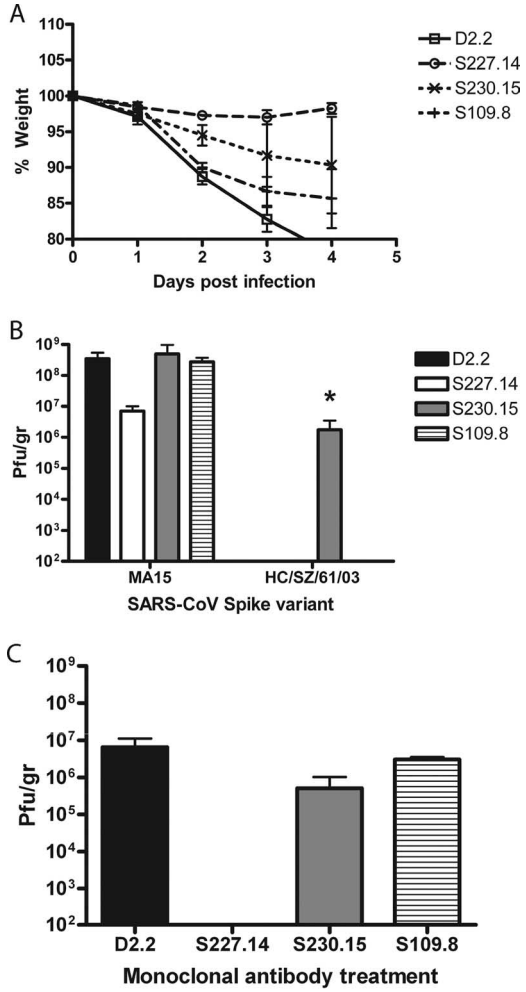

FIG. 5. Prophylactic treatment of lethal SARS-CoV infections in 10-week-old BALB/c mice with 25 μg of cross-neutralizing MAbs. (A) Body weights of mice infected with MA15 were measured daily after passive transfer of 25 μg of MAb S109.8 (+), S227.14 (○), S230.15 (×), or D2.2 (□). (B) Lung tissues of mice infected with MA15 or icHC/SZ/61/03 were harvested on day 2 postinfection and assayed for infectious virus. (C) Lung tissues of mice infected with MA15 were harvested on day 4 postinfection and assayed for infectious virus. Error bars, standard deviations ($n = 3$). *, only one animal out of three had detectable virus titers.

The recent development of a mouse-adapted SARS-CoV variant (icMA15) (33) allowed us to test MAb effectiveness against a homologous lethal challenge virus in young mice. The MA15 virus has a single mouse-adapted change in the S glycoprotein at residue Y436H. Ten-week-old BALB/c mice that received 25 μg of S227.14 were significantly and completely protected against weight loss after challenge with icMA15 (Fig. 5A). Animals that received either S230.15 or S109.8 all had significant weight loss starting by day 3 or 2 postinfection, respectively ($P < 0.01$ by the t test), with a maximum of 15%, but eventually leveled out by day 4 (Fig. 5A). Virus titers in the lungs of animals that received S227.14 were lower on day 2 than those for animals that received either S230.15, S109.8, or the D2.2 control (Fig. 5B). Interestingly, on day 4, no virus could be detected in the lungs of animals treated with S227.14 (Fig. 5C).

Postinfection treatment of lethal challenge. Given the possibility of lethal infection and community spread, antibody prophylaxis following SARS-CoV exposure is an important public health consideration, especially for laboratory personnel. Therefore, one of the most efficient cross-neutralizing MAbs, S230.15, was used prophylactically at a dose of 250 μg at different times after exposure with icGZ02 in an aged-mouse infection model. Complete protection from weight loss was observed when 12-month-old BALB/c mice were immunized 1 day prior to challenge (Fig. 6A). Mice immunized at the time of infection lost up to 10% of their weight by day 2 postchallenge ($P < 0.01$ by the t test) but recovered by day 3. Treatment of BALB/c mice at 1, 2, or 3 days postchallenge did not protect against weight loss, suggesting a narrow window of prophylactic activity in the mouse model of acute lethal challenge (Fig. 6A).

Virus titers in the lungs were examined on days 2 and 4. By day 2 postchallenge, complete protection against virus replication in the lungs of BALB/c mice treated with the MAb 1 day prior to challenge was observed ($P < 0.01$ by ANOVA) (Fig. 6B). In contrast, a 5-log-unit reduction in virus titers was observed when mice were treated on the day of challenge (detectable virus in only one out of four animals; $P < 0.01$ by ANOVA). Consistent with the development of severe clinical disease, no reduction in viral titers was observed when mice were treated 1 day postchallenge (Fig. 6B). By day 4 postchallenge, virus was no longer detectable in the lungs of mice treated 1 day prior to challenge, on the day of challenge, or 2 or 3 days postchallenge ($P < 0.01$ by ANOVA), and virus was

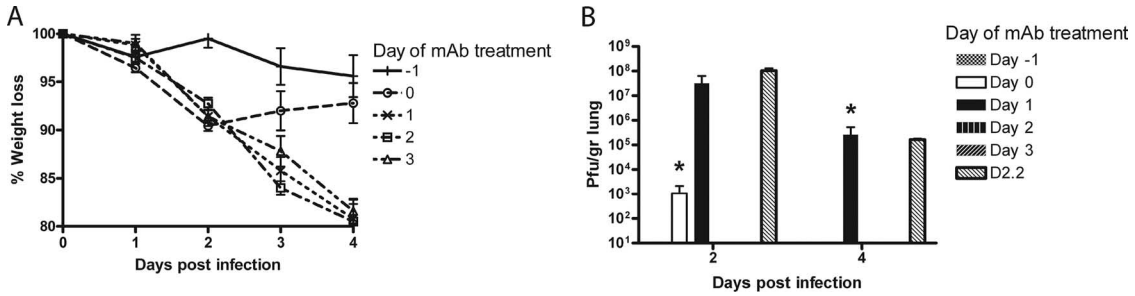

FIG. 6. Postinfection treatment of 12-month-old BALB/c mice infected with SARS-CoV. (A) Body weights of mice infected with GZ02 were measured daily after passive transfer of 250 μg of MAb S230.15 at day −1 (+), day 0 (○), or day 1 (×), 2 (□), or 3(△) postinfection. (B) Lung tissues of mice infected with GZ02 were harvested on days 2 and 4 postinfection and were assayed for infectious virus. Error bars, standard deviations ($n = 5$). *, only one animal out of five had detectable virus titers.

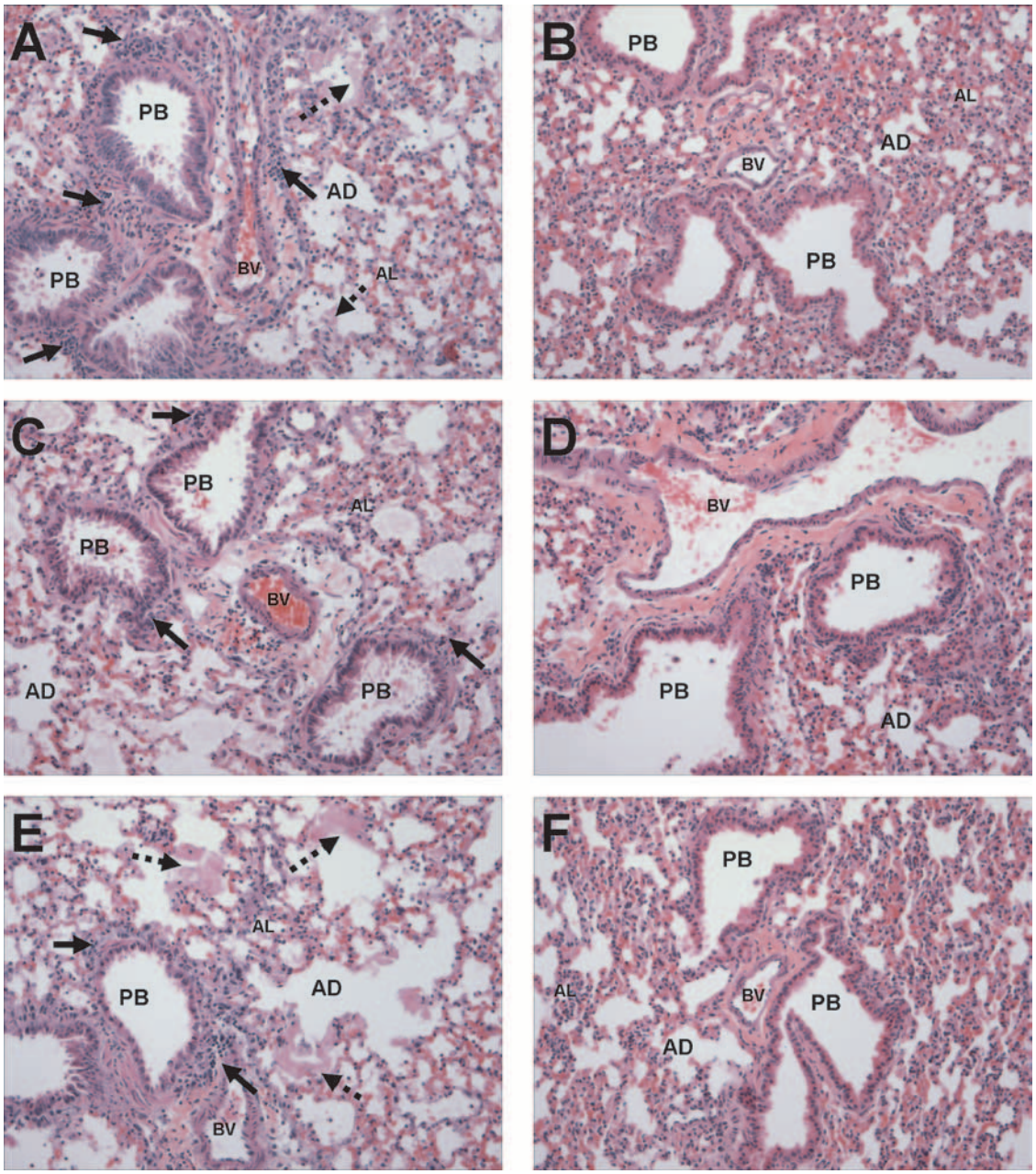

FIG. 7. Light photographs of preterminal bronchioles (PB) in the lungs of 12-month-old BALB/c mice that had received 250 μg of a human MAb prior to SARS-CoV infection and were sacrificed 5 days postinoculation. Virus-induced peribronchiolar inflammation (solid arrows) is evident in mice treated with the control MAb D2.2 and infected with icUrbani (A), icGZ02 (C), or icHC/SZ/61/03 (E). Numerous hyaline membranes (dashed arrows) are present in the alveolar airspaces of mice treated with the control MAb. No inflammation or hyaline membrane formation can be observed in mice treated with 250 μg of S230.15 and subsequently infected with icUrbani (B), icGZ02 (D), or icHC/SZ/61/03 (F). AL, alveoli; AD, alveolar ducts; BV, blood vessels. Tissues were stained with hematoxylin and eosin. Magnification, ×100.

detectable only in one out of five BALB/c mice treated with the MAb on day 1 postchallenge (Fig. 6B).

These data suggest that the lethal course of SARS-CoV infection in the mouse model may well be set within the first 24 h postinfection, since this MAb was not capable of reversing the severity of clinical disease.

Pathological findings. The recapitulation in BALB/c mice of the age-related pathology observed in acute cases of SARS-CoV infection in humans (37) provides us with a third measure of protection along with morbidity and viral titers. Although there was some animal-to-animal variation, in general 12-month-old BALB/c mice that received the control MAb D2.2 showed evidence of bronchiolitis with epithelial cell exfoliation, virus-induced peribronchiolar inflammation, diffuse acute alveolitis, and numerous hyaline membranes in the alveolar airspaces after infection with icUrbani (Fig. 7A), icGZ02 (Fig. 7C), or icHC/SZ/61/03 (Fig. 7E). Animals that received 250 μg of either MAb 230.15 (Fig. 7B, D, and F) or a cocktail of MAbs

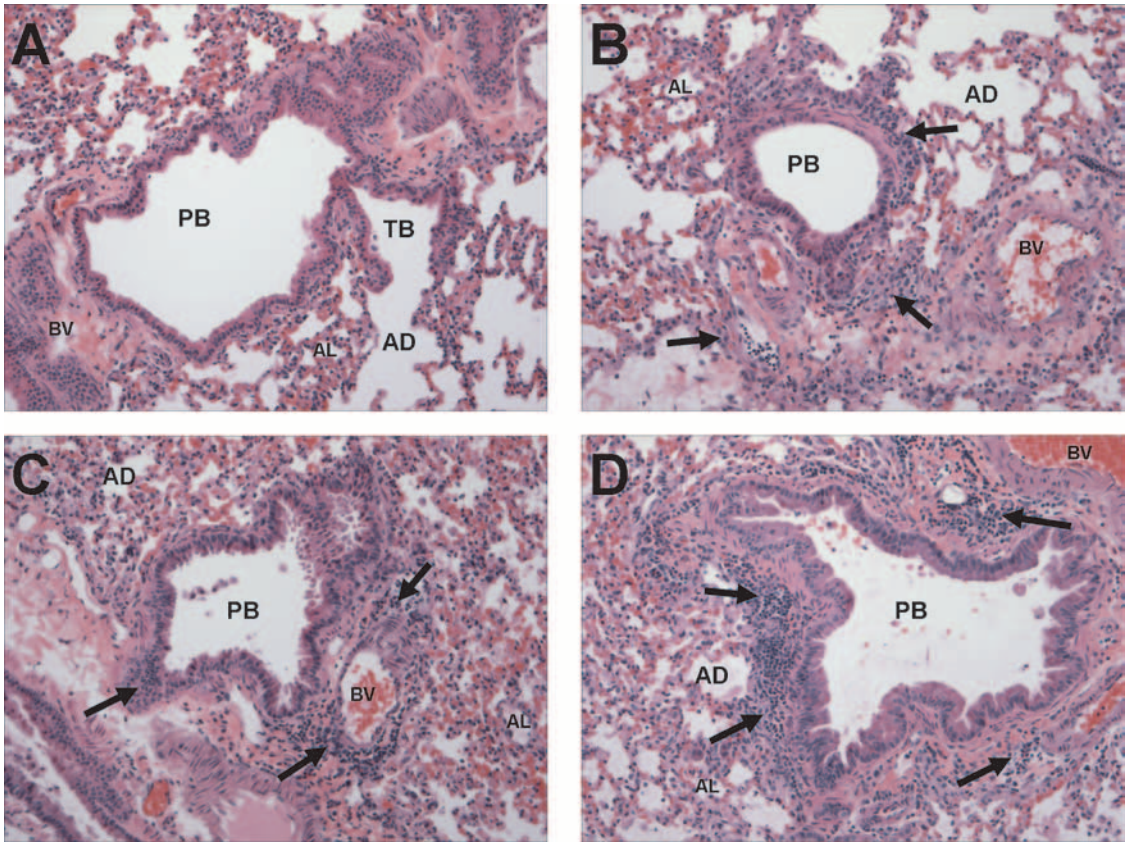

FIG. 8. Light photographs of preterminal bronchioles (PB) and terminal bronchioles (TB) in the lungs of 12-month-old BALB/c mice that received 250 μg of a human MAb after infection with SARS-CoV and were sacrificed 5 days postinoculation. (A) No inflammation or hyaline membrane formation can be observed in mice treated with 250 μg of S230.15 on the day of infection with icGZ02. (B through D) Increasing-virus induced peribronchiolar inflammation (solid arrows) is evident in mice treated with 250 μg of MAb S230.15 at day 1 (B), 2 (C), or 3 (D) postinfection. AL, alveoli; AD, alveolar ducts; BV, blood vessels. Tissues were stained with hematoxylin and eosin. Magnification, ×100.

S109.8, S227.14, and S230.15 (data not shown) before infection showed marked decreases in bronchiolitis, exfoliation, and alveolar inflammation, and hyaline membrane formation was absent. No clear decrease in alveolar inflammation or bronchiolitis was observed when animals received 25 μg of either MAb 230.15 or the cocktail; however, animals were protected against hyaline membrane formation (data not shown). Finally, in agreement with the morbidity data, mice showed clear reductions in pathological changes only when they were treated with the MAb 1 day prior to the day of infection (Fig. 7D) or on the day of infection (Fig. 8A), not when they were treated on day 1, 2, or 3 postinfection (Fig. 8B, C, and D, respectively). No evidence of enhanced disease or pathology was observed with any of the MAbs or any of the challenge viruses.

DISCUSSION

SARS-CoV is a newly emergent human respiratory pathogen that caused a major outbreak in community settings around the world in 2002 to 2003. Several laboratory-acquired cases have been reported with subsequent spread of the disease into communities, resulting in additional outbreaks in 2003 to 2004 (25, 31). Since these epidemics, no human cases have been reported, and epidemic human strains are believed to be extinct. However, several SARS-CoV strains have been sequenced from possible zoonotic reservoirs, including palm civets, raccoon dogs, and bats, and new human strains will likely evolve from these reservoirs (11, 23). In support of this hypothesis, we have shown that many of these animal strains encode an S glycoprotein that can utilize human ACE2 for docking and entry (37). Additionally, the SARS-CoV infections involving researchers underscore the need for medical countermeasures for postexposure prophylaxis. Therefore, protection against zoonotic and early human-to-human transmission, especially in more vulnerable elderly populations, should receive high priority (3, 5, 36).

The goal of this study was to identify and characterize cross-neutralizing human MAbs that efficiently neutralize an extensive panel of variant SARS-CoV isolates bearing S glycoproteins from both the human and the zoonotic phases of the epidemic (37). For the first time, we evaluated the use of human MAbs in the prevention and treatment of lethal homologous and heterologous SARS-CoV infections in murine models. Uniquely, this study not only carefully mapped the cross-reactive neutralization effectiveness of a large panel of human MAbs against human and zoonotic isolates but also identified at least three MAbs that recognize unique epitopes and neutralize all SARS-CoV isolates tested in vitro and in

vivo. A similar strategy has recently been used to identify cross-reactive protective human MAbs against influenza virus H5N1 (41).

Several studies have shown that the generation of neutralizing antibodies against SARS-CoV is a major component of protective immunity (47, 48). A few studies have focused on evaluating the cross-neutralizing potential of human and murine antibodies and have measured cross-neutralization indexes using a small number of pseudotyped viruses bearing S glycoproteins from SARS-CoV isolates throughout the epidemic (12, 56). These studies have demonstrated mixed results ranging from no cross-neutralization to enhanced infection and even robust cross-neutralization, complicating the interpretation of data.

Given the variable responses reported with pseudotyped viruses (30, 55), we used an isogenic panel of recombinant SARS-CoVs bearing variant human epidemic and zoonotic S glycoproteins to evaluate the role of S glycoprotein heterogeneity in neutralization by MAbs (37). Using this panel of viruses, we identified 23 human MAbs that effectively neutralized one or multiple SARS-CoV S isolates, dividing the antibodies into six distinct neutralizing categories. More importantly, we identified four MAbs that efficiently neutralize both human and zoonotic SARS-CoV isolates. MAb S230.15 has recently been shown to have cross-neutralizing in vitro and in vivo activities against GD03-S and SZ16-K479N recombinant viruses (57); however, we expanded on these studies to include several more MAbs and three more SARS-CoV spike isolates as well as mapping of the putative epitopes.

In agreement with previous studies, sequence analysis, competition studies, and inhibition of SARS-CoV S binding to ACE2 showed that the majority of our panel of MAbs recognized epitopes within the RBD, with the exception of two MAbs (S132 and S228.11, constituting group I) that likely recognize epitopes in the N terminus of the S1 domain. The majority of the human MAbs (groups III and IV) likely recognize a set of overlapping conformational epitopes, since reactivity was lost by denaturation of the antigen, as seen with the hepatitis B virus surface antigen (38).

At least three of the cross-neutralizing MAbs (S109.8, S230.15, and S227.14) were mapped within the RBD. Since S230.15 and S227.14 compete with S215.17, all the cross-neutralizing antibodies likely map in the RBD. The epitope of MAb S230.15 likely overlaps with the epitopes that were recognized by 80R and m396, since at least one amino acid (aa 487) was identified as an important residue both for S230.15 and for 80R and m396 (15, 32, 43). MAb S227.14 was shown to recognize an epitope that partially overlapped with the S230.15 epitope but is likely distinct from the 80R and m396 epitopes. Recognition of partially overlapping but distinct epitopes has also been reported for other viruses, including human immunodeficiency virus type 1 and hepatitis A virus (18, 29). Although MAb S109.8 likely recognizes an epitope within the RBD, the site is located away from residues in direct contact with ACE2. The mechanism of neutralization by S109.8 is unknown, but we hypothesize that binding of S109.8 to the RBD may result in either structural changes that affect its binding to ACE2, blocking of structural changes in the RBD needed for efficient binding to ACE2, or steric hindrance during ACE2 binding, as has been described for poliovirus, avian sarcoma-leukosis virus, and human papillomavirus (7, 53, 54).

The locations and mechanisms of neutralization for the other MAbs identified in this study remain unknown, underscoring the need for more-detailed analysis of escape mutants and the efficacy of protection in vivo.

We successfully used escape mutant analysis to identify key residues involved in the neutralizing activities of two cross-neutralizing human MAbs. Escape variant analysis has been used previously to identify the importance of P462 in the neutralization of SARS-CoV by MAb CR3014 (46) as well as to identify epitopes for various other viruses, including influenza virus (17). Although escape mutants can be helpful in identifying important neutralizing residues, they compromise the use of the MAb as prophylaxis or treatment. Previous studies with human MAbs neutralizing SARS-CoV and rabies virus have shown that the use of a MAb cocktail may circumvent this problem (2, 46). Our data show that individual MAb escape mutants can be efficiently neutralized by the other cross-neutralizing MAbs and that these MAbs should therefore be used as a cocktail to prevent the generation of escape mutants. This application is especially useful given that we were unsuccessful in isolating neutralization escape mutants against one of the MAbs (S227.14).

The use of neutralizing MAbs in passive immunizations has been well established (27, 39). This form of immunization has the advantage of providing immediate protection in the absence of a humoral immune response and may be especially advantageous for elderly populations, since they show increased morbidity and mortality caused by infectious diseases in general and SARS-CoV in particular (1, 4, 5, 44). This is generally accepted to be due to a compromised senescent immune system (1, 44), as demonstrated by the limited protection against a heterologous SARS-CoV in vaccinated aged mice (8). Therefore, the use of MAbs shown to cross-neutralize human and zoonotic SARS-CoV strains may be an attractive alternative for use in the elderly as well as in laboratory personnel after accidental exposure.

Several studies have shown that MAbs and polyclonal sera can effectively protect young mice from homologous SARS-CoV replication in the lung (42, 43). These models evaluated virus replication only in the absence of clinical disease, and the aged-mouse model recapitulating human SARS-CoV infection allows a more relevant evaluation of efficacy (34). We recently developed lethal models of SARS-CoV bearing variant S glycoproteins that recapitulated the age-related highly pathogenic phenotype observed in acute SARS cases in humans (37). Aged mice have been used to test whether immune serum protects from weight loss, reduces viral titers, and prevents histopathologic changes in the lungs (51). However, to date no MAbs have been tested in aged-animal models of SARS-CoV, especially following heterologous challenge with lethal viruses. These models have the advantage of testing treatment regimens in the most vulnerable populations, the elderly, as well as generally evaluating the efficacy of immunoprophylactic therapy in this population.

In the present study, we tested the abilities of three broad-spectrum human MAbs to cross-protect against challenge with one homologous and three heterologous SARS-CoV isolates. We showed complete protection against clinical disease and

virus replication in the lungs of mice treated with S227.14 or S230.15 and challenged with a late- or early-phase human isolate. Interestingly, animals were also protected against clinical disease after challenge with the palm civet isolate despite the presence of high viral titers in the lung. Although animals were not completely protected against viral replication on day 2 postinfection, no virus could be detected by day 5, thereby reducing the chance of transmission. A cocktail of multiple MAbs was as capable of protecting against lethal challenge as the most potent individual MAbs, providing a strategy for minimizing the emergence of MAb escape mutants (2, 46).

Aged animals were less effective at clearing heterologous virus than were the younger animals. This may be due to an impaired innate immune system in the elderly (1) or to differences in the efficiency of the human MAbs at reaching the lung mucosa and neutralizing the virus. Bidirectional IgG transport across epithelial barriers is mediated in part by the major histocompatibility complex class I-related Fc receptor, which has been shown to be downregulated by age (9). To our knowledge, this is the first study to compare and document differences in passive immunization efficacy between young and aged animals, potentially documenting an important clinical consideration in the treatment of the elderly. The effect of age on the efficacy of passive immunizations should be studied in further detail, perhaps by evaluating antibody efficacy in progressively older animals challenged with lethal viruses.

Ideally, these antibodies could also be used in postinfection treatment of SARS-CoV. MAb S230.15 could effectively protect against or reduce the clinical symptoms of SARS-CoV infection only when mice were treated with the MAb 1 day prior to challenge or on the day of challenge. This was particularly surprising because similar treatments were very successful with H5N1 influenza virus infections in mice (41). However, we used a much higher dose of SARS-CoV to challenge the mice, and the SARS-CoV infection models are much more acute than the model of influenza virus H5N1 infection in mice. In addition, the murine Fc receptor has a relatively low affinity for the human Fc portion, which may also explain the difference in protection between S230.15 and S227.14 in young mice challenged with the highly lethal MA15 virus. Therefore, future experiments to assess the role of the Fc portion in the effector neutralizing potential of the MAbs may be necessary. Interestingly, mice treated at 2 or 3 days postchallenge did reduce viral loads by clearing virus replication by day 4, but these animals were not protected against clinical disease. These data suggest that the clinical disease course is set within the first 24 h of infection, since mice were not protected with MAbs after this time and died even after virus had been cleared. This is in agreement with observations of human SARS cases, where a large subset of cases showed clinical disease after virus clearance (14).

Our data show that cross-reacting MAbs exist that can efficiently neutralize all human and zoonotic SARS-CoV isolates reported to date. It is interesting that broadly neutralizing MAbs were isolated at a late time point after infection (2 years), suggesting a long-lasting maintenance of potent SARS-CoV-neutralizing MAbs in the B-cell memory repertoire, which would protect survivors against epidemic and zoonotic SARS-CoV emergence. While escape mutants could be generated against some of the MAbs, these could still be neutralized by the other MAbs, stressing the importance of combination therapy. In addition, we showed that escape mutant analysis coupled with a time-ordered panel of outbreak isolates provides a novel set of reagents with which to map neutralizing epitopes. These methods can potentially be used to identify and characterize cross-neutralizing epitopes of novel emerging viral pathogens. Cross-neutralizing epitopes will be important targets for the development of a vaccine that protects against the reemergence of SARS-CoV from its zoonotic reservoir. These MAbs are attractive candidates for prophylactic treatment of SARS-CoV infection, and further development should include testing in larger-animal models of SARS-CoV infection such as ferrets and nonhuman primates, including transmission models. We also showed the importance of testing multiple heterologous SARS-CoV strains and the use of robust animal models with multiple readouts, e.g., virus replication, pathology, clinical signs, and mortality. These models will be essential for successful vaccine development in aged populations. Finally, understanding the mechanisms of neutralization may provide insight into the SARS-CoV entry process.

ACKNOWLEDGMENTS

This work was supported by NIH grants P01-AI059443 and P01-AI059136 and by the European Union SARSVAC grant N. SP22.CT.2004.511065.

REFERENCES

1. **Aw, D., A. B. Silva, and D. B. Palmer.** 2007. Immunosenescence: emerging challenges for an ageing population. Immunology **120:**435–446.
2. **Bakker, A. B., W. E. Marissen, R. A. Kramer, A. B. Rice, W. C. Weldon, M. Niezgoda, C. A. Hanlon, S. Thijsse, H. H. Backus, J. de Kruif, B. Dietzschold, C. E. Rupprecht, and J. Goudsmit.** 2005. Novel human monoclonal antibody combination effectively neutralizing natural rabies virus variants and individual in vitro escape mutants. J. Virol. **79:**9062–9068.
3. **Baric, R. S., T. Sheahan, D. Deming, E. Donaldson, B. Yount, A. C. Sims, R. S. Roberts, M. Frieman, and B. Rockx.** 2006. SARS coronavirus vaccine development. Adv. Exp. Med. Biol. **581:**553–560.
4. **Chan, K. C., N. L. Tang, D. S. Hui, G. T. Chung, A. K. Wu, S. S. Chim, R. W. Chiu, N. Lee, K. W. Choi, Y. M. Sung, P. K. Chan, Y. K. Tong, S. T. Lai, W. C. Yu, O. Tsang, and Y. M. Lo.** 2005. Absence of association between angiotensin converting enzyme polymorphism and development of adult respiratory distress syndrome in patients with severe acute respiratory syndrome: a case control study. BMC Infect. Dis. **5:**26.
5. **Chan-Yeung, M., and R. H. Xu.** 2003. SARS: epidemiology. Respirology **8**(Suppl.)**:**S9–S14.
6. **Chinese SARS Molecular Epidemiology Consortium.** 2004. Molecular evolution of the SARS coronavirus during the course of the SARS epidemic in China. Science **303:**1666–1669.
7. **Day, P. M., C. D. Thompson, C. B. Buck, Y. Y. Pang, D. R. Lowy, and J. T. Schiller.** 2007. Neutralization of human papillomavirus with monoclonal antibodies reveals different mechanisms of inhibition. J. Virol. **81:**8784–8792.
8. **Deming, D., T. Sheahan, M. Heise, B. Yount, N. Davis, A. Sims, M. Suthar, J. Harkema, A. Whitmore, R. Pickles, A. West, E. Donaldson, K. Curtis, R. Johnston, and R. Baric.** 2006. Vaccine efficacy in senescent mice challenged with recombinant SARS-CoV bearing epidemic and zoonotic spike variants. PLoS Med. **3:**e525.
9. **Dickinson, B. L., K. Badizadegan, Z. Wu, J. C. Ahouse, X. Zhu, N. E. Simister, R. S. Blumberg, and W. I. Lencer.** 1999. Bidirectional FcRn-dependent IgG transport in a polarized human intestinal epithelial cell line. J. Clin. Investig. **104:**903–911.
10. **Greenough, T. C., G. J. Babcock, A. Roberts, H. J. Hernandez, W. D. Thomas, Jr., J. A. Coccia, R. F. Graziano, M. Srinivasan, I. Lowy, R. W. Finberg, K. Subbarao, L. Vogel, M. Somasundaran, K. Luzuriaga, J. L. Sullivan, and D. M. Ambrosino.** 2005. Development and characterization of a severe acute respiratory syndrome-associated coronavirus-neutralizing human monoclonal antibody that provides effective immunoprophylaxis in mice. J. Infect. Dis. **191:**507–514.
11. **Guan, Y., B. J. Zheng, Y. Q. He, X. L. Liu, Z. X. Zhuang, C. L. Cheung, S. W. Luo, P. H. Li, L. J. Zhang, Y. J. Guan, K. M. Butt, K. L. Wong, K. W. Chan, W. Lim, K. F. Shortridge, K. Y. Yuen, J. S. Peiris, and L. L. Poon.** 2003. Isolation and characterization of viruses related to the SARS coronavirus from animals in southern China. Science **302:**276–278.

12. **He, Y., J. Li, W. Li, S. Lustigman, M. Farzan, and S. Jiang.** 2006. Cross-neutralization of human and palm civet severe acute respiratory syndrome coronaviruses by antibodies targeting the receptor-binding domain of spike protein. J. Immunol. **176:**6085–6092.
13. **He, Y., Y. Zhou, S. Liu, Z. Kou, W. Li, M. Farzan, and S. Jiang.** 2004. Receptor-binding domain of SARS-CoV spike protein induces highly potent neutralizing antibodies: implication for developing subunit vaccine. Biochem. Biophys. Res. Commun. **324:**773–781.
14. **Huang, K. J., I. J. Su, M. Theron, Y. C. Wu, S. K. Lai, C. C. Liu, and H. Y. Lei.** 2005. An interferon-gamma-related cytokine storm in SARS patients. J. Med. Virol. **75:**185–194.
15. **Hwang, W. C., Y. Lin, E. Santelli, J. Sui, L. Jaroszewski, B. Stec, M. Farzan, W. A. Marasco, and R. C. Liddington.** 2006. Structural basis of neutralization by a human anti-severe acute respiratory syndrome spike protein antibody, 80R. J. Biol. Chem. **281:**34610–34616.
16. **Kan, B., M. Wang, H. Jing, H. Xu, X. Jiang, M. Yan, W. Liang, H. Zheng, K. Wan, Q. Liu, B. Cui, Y. Xu, E. Zhang, H. Wang, J. Ye, G. Li, M. Li, Z. Cui, X. Qi, K. Chen, L. Du, K. Gao, Y. T. Zhao, X. Z. Zou, Y. J. Feng, Y. F. Gao, R. Hai, D. Yu, Y. Guan, and J. Xu.** 2005. Molecular evolution analysis and geographic investigation of severe acute respiratory syndrome coronavirus-like virus in palm civets at an animal market and on farms. J. Virol. **79:** 11892–11900.
17. **Kaverin, N. V., I. A. Rudneva, N. A. Ilyushina, N. L. Varich, A. S. Lipatov, Y. A. Smirnov, E. A. Govorkova, A. K. Gitelman, D. K. Lvov, and R. G. Webster.** 2002. Structure of antigenic sites on the haemagglutinin molecule of H5 avian influenza virus and phenotypic variation of escape mutants. J. Gen. Virol. **83:**2497–2505.
18. **Kim, S. J., M. H. Jang, J. T. Stapleton, S. O. Yoon, K. S. Kim, E. S. Jeon, and H. J. Hong.** 2004. Neutralizing human monoclonal antibodies to hepatitis A virus recovered by phage display. Virology **318:**598–607.
19. **Kuiken, T., R. A. Fouchier, M. Schutten, G. F. Rimmelzwaan, G. van Amerongen, D. van Riel, J. D. Laman, T. de Jong, G. van Doornum, W. Lim, A. E. Ling, P. K. Chan, J. S. Tam, M. C. Zambon, R. Gopal, C. Drosten, S. van der Werf, N. Escriou, J. C. Manuguerra, K. Stohr, J. S. Peiris, and A. D. Osterhaus.** 2003. Newly discovered coronavirus as the primary cause of severe acute respiratory syndrome. Lancet **362:**263–270.
20. **Lai, S. C., P. C. Chong, C. T. Yeh, L. S. Liu, J. T. Jan, H. Y. Chi, H. W. Liu, A. Chen, and Y. C. Wang.** 2005. Characterization of neutralizing monoclonal antibodies recognizing a 15-residues epitope on the spike protein HR2 region of severe acute respiratory syndrome coronavirus (SARS-CoV). J. Biomed. Sci. **12:**711–727.
21. **Li, F., W. Li, M. Farzan, and S. C. Harrison.** 2005. Structure of SARS coronavirus spike receptor-binding domain complexed with receptor. Science **309:**1864–1868.
22. **Li, W., M. J. Moore, N. Vasilieva, J. Sui, S. K. Wong, M. A. Berne, M. Somasundaran, J. L. Sullivan, K. Luzuriaga, T. C. Greenough, H. Choe, and M. Farzan.** 2003. Angiotensin-converting enzyme 2 is a functional receptor for the SARS coronavirus. Nature **426:**450–454.
23. **Li, W., Z. Shi, M. Yu, W. Ren, C. Smith, J. H. Epstein, H. Wang, G. Crameri, Z. Hu, H. Zhang, J. Zhang, J. McEachern, H. Field, P. Daszak, B. T. Eaton, S. Zhang, and L. F. Wang.** 2005. Bats are natural reservoirs of SARS-like coronaviruses. Science **310:**676–679.
24. **Li, W., C. Zhang, J. Sui, J. H. Kuhn, M. J. Moore, S. Luo, S. K. Wong, I. C. Huang, K. Xu, N. Vasilieva, A. Murakami, Y. He, W. A. Marasco, Y. Guan, H. Choe, and M. Farzan.** 2005. Receptor and viral determinants of SARS-coronavirus adaptation to human ACE2. EMBO J. **24:**1634–1643.
25. **Lim, P. L., A. Kurup, G. Gopalakrishna, K. P. Chan, C. W. Wong, L. C. Ng, S. Y. Se-Thoe, L. Oon, X. Bai, L. W. Stanton, Y. Ruan, L. D. Miller, V. B. Vega, L. James, P. L. Ooi, C. S. Kai, S. J. Olsen, B. Ang, and Y. S. Leo.** 2004. Laboratory-acquired severe acute respiratory syndrome. N. Engl. J. Med. **350:**1740–1745.
26. **Liu, M., W. N. Liang, Q. Chen, X. Q. Xie, J. Wu, X. He, and Z. J. Liu.** 2006. Risk factors for SARS-related deaths in 2003, Beijing. Biomed. Environ. Sci. **19:**336–339.
27. **Marasco, W. A., and J. Sui.** 2007. The growth and potential of human antiviral monoclonal antibody therapeutics. Nat. Biotechnol. **25:**1421–1434.
28. **Moore, J. P., and J. Sodroski.** 1996. Antibody cross-competition analysis of the human immunodeficiency virus type 1 gp120 exterior envelope glycoprotein. J. Virol. **70:**1863–1872.
29. **Nelson, J. D., F. M. Brunel, R. Jensen, E. T. Crooks, R. M. Cardoso, M. Wang, A. Hessell, I. A. Wilson, J. M. Binley, P. E. Dawson, D. R. Burton, and M. B. Zwick.** 2007. An affinity-enhanced neutralizing antibody against the membrane-proximal external region of human immunodeficiency virus type 1 gp41 recognizes an epitope between those of 2F5 and 4E10. J. Virol. **81:**4033–4043.
30. **Nie, Y., G. Wang, X. Shi, H. Zhang, Y. Qiu, Z. He, W. Wang, G. Lian, X. Yin, L. Du, L. Ren, J. Wang, X. He, T. Li, H. Deng, and M. Ding.** 2004. Neutralizing antibodies in patients with severe acute respiratory syndrome-associated coronavirus infection. J. Infect. Dis. **190:**1119–1126.
31. **Orellana, C.** 2004. Laboratory-acquired SARS raises worries on biosafety. Lancet Infect. Dis. **4:**64.
32. **Prabakaran, P., J. Gan, Y. Feng, Z. Zhu, V. Choudhry, X. Xiao, X. Ji, and D. S. Dimitrov.** 2006. Structure of severe acute respiratory syndrome coronavirus receptor-binding domain complexed with neutralizing antibody. J. Biol. Chem. **281:**15829–15836.
33. **Roberts, A., D. Deming, C. D. Paddock, A. Cheng, B. Yount, L. Vogel, B. D. Herman, T. Sheahan, M. Heise, G. L. Genrich, S. R. Zaki, R. Baric, and K. Subbarao.** 2007. A mouse-adapted SARS-coronavirus causes disease and mortality in BALB/c mice. PLoS Pathog. **3:**e5.
34. **Roberts, A., C. Paddock, L. Vogel, E. Butler, S. Zaki, and K. Subbarao.** 2005. Aged BALB/c mice as a model for increased severity of severe acute respiratory syndrome in elderly humans. J. Virol. **79:**5833–5838.
35. **Roberts, A., W. D. Thomas, J. Guarner, E. W. Lamirande, G. J. Babcock, T. C. Greenough, L. Vogel, N. Hayes, J. L. Sullivan, S. Zaki, K. Subbarao, and D. M. Ambrosino.** 2006. Therapy with a severe acute respiratory syndrome-associated coronavirus-neutralizing human monoclonal antibody reduces disease severity and viral burden in golden Syrian hamsters. J. Infect. Dis. **193:**685–692.
36. **Rockx, B., and R. S. Baric.** 2007. Grand challenges in human coronavirus vaccine development, p. 257–286. *In* V. Thiel (ed.), Coronaviruses: molecular and cellular biology. Caister Academic Press, Norfolk, United Kingdom.
37. **Rockx, B., T. Sheahan, E. Donaldson, J. Harkema, A. Sims, M. Heise, R. Pickles, M. Cameron, D. Kelvin, and R. Baric.** 2007. Synthetic reconstruction of zoonotic and early human severe acute respiratory syndrome coronavirus isolates that produce fatal disease in aged mice. J. Virol. **81:**7410–7423.
38. **Roohi, A., J. Khoshnoodi, A. H. Zarnani, and F. Shokri.** 2005. Epitope mapping of recombinant hepatitis B surface antigen by murine monoclonal antibodies. Hybridoma (Larchmont) **24:**71–77.
39. **Sawyer, L. A.** 2000. Antibodies for the prevention and treatment of viral diseases. Antivir. Res. **47:**57–77.
40. **Sheng, W. H., B. L. Chiang, S. C. Chang, H. N. Ho, J. T. Wang, Y. C. Chen, C. H. Hsiao, P. R. Hseuh, W. C. Chie, and P. C. Yang.** 2005. Clinical manifestations and inflammatory cytokine responses in patients with severe acute respiratory syndrome. J. Formos. Med. Assoc. **104:**715–723.
41. **Simmons, C. P., N. L. Bernasconi, A. L. Suguitan, K. Mills, J. M. Ward, N. V. Chau, T. T. Hien, F. Sallusto, D. Q. Ha, J. Farrar, M. D. de Jong, A. Lanzavecchia, and K. Subbarao.** 2007. Prophylactic and therapeutic efficacy of human monoclonal antibodies against H5N1 influenza. PLoS Med. **4:**e178.
42. **Subbarao, K., J. McAuliffe, L. Vogel, G. Fahle, S. Fischer, K. Tatti, M. Packard, W. J. Shieh, S. Zaki, and B. Murphy.** 2004. Prior infection and passive transfer of neutralizing antibody prevent replication of severe acute respiratory syndrome coronavirus in the respiratory tract of mice. J. Virol. **78:**3572–3577.
43. **Sui, J., W. Li, A. Roberts, L. J. Matthews, A. Murakami, L. Vogel, S. K. Wong, K. Subbarao, M. Farzan, and W. A. Marasco.** 2005. Evaluation of human monoclonal antibody 80R for immunoprophylaxis of severe acute respiratory syndrome by an animal study, epitope mapping, and analysis of spike variants. J. Virol. **79:**5900–5906.
44. **Targonski, P. V., R. M. Jacobson, and G. A. Poland.** 2007. Immunosenescence: role and measurement in influenza vaccine response among the elderly. Vaccine **25:**3066–3069.
45. **ter Meulen, J., A. B. Bakker, E. N. van den Brink, G. J. Weverling, B. E. Martina, B. L. Haagmans, T. Kuiken, J. de Kruif, W. Preiser, W. Spaan, H. R. Gelderblom, J. Goudsmit, and A. D. Osterhaus.** 2004. Human monoclonal antibody as prophylaxis for SARS coronavirus infection in ferrets. Lancet **363:**2139–2141.
46. **ter Meulen, J., E. N. van den Brink, L. L. Poon, W. E. Marissen, C. S. Leung, F. Cox, C. Y. Cheung, A. Q. Bakker, J. A. Bogaards, E. van Deventer, W. Preiser, H. W. Doerr, V. T. Chow, J. de Kruif, J. S. Peiris, and J. Goudsmit.** 2006. Human monoclonal antibody combination against SARS coronavirus: synergy and coverage of escape mutants. PLoS Med. **3:**e237.
47. **Traggiai, E., S. Becker, K. Subbarao, L. Kolesnikova, Y. Uematsu, M. R. Gismondo, B. R. Murphy, R. Rappuoli, and A. Lanzavecchia.** 2004. An efficient method to make human monoclonal antibodies from memory B cells: potent neutralization of SARS coronavirus. Nat. Med. **10:**871–875.
48. **Tripp, R. A., L. M. Haynes, D. Moore, B. Anderson, A. Tamin, B. H. Harcourt, L. P. Jones, M. Yilla, G. J. Babcock, T. Greenough, D. M. Ambrosino, R. Alvarez, J. Callaway, S. Cavitt, K. Kamrud, H. Alterson, J. Smith, J. L. Harcourt, C. Miao, R. Razdan, J. A. Comer, P. E. Rollin, T. G. Ksiazek, A. Sanchez, P. A. Rota, W. J. Bellini, and L. J. Anderson.** 2005. Monoclonal antibodies to SARS-associated coronavirus (SARS-CoV): identification of neutralizing and antibodies reactive to S, N, M and E viral proteins. J. Virol. Methods **128:**21–28.
49. **Tzartos, S. J.** 1996. Epitope mapping by antibody competition. Methodology and evaluation of the validity of the technique. Methods Mol. Biol. **66:**55–66.
50. **Vicenzi, E., F. Canducci, D. Pinna, N. Mancini, S. Carletti, A. Lazzarin, C. Bordignon, G. Poli, and M. Clementi.** 2004. *Coronaviridae* and SARS-associated coronavirus strain HSR1. Emerg. Infect. Dis. **10:**413–418.
51. **Vogel, L. N., A. Roberts, C. D. Paddock, G. L. Genrich, E. W. Lamirande, S. U. Kapadia, J. K. Rose, S. R. Zaki, and K. Subbarao.** 2007. Utility of the aged BALB/c mouse model to demonstrate prevention and control strategies

for severe acute respiratory syndrome coronavirus (SARS-CoV). Vaccine **25:**2173–2179.

52. **Wang, P., J. Chen, A. Zheng, Y. Nie, X. Shi, W. Wang, G. Wang, M. Luo, H. Liu, L. Tan, X. Song, Z. Wang, X. Yin, X. Qu, X. Wang, T. Qing, M. Ding, and H. Deng.** 2004. Expression cloning of functional receptor used by SARS coronavirus. Biochem. Biophys. Res. Commun. **315:**439–444.
53. **Wien, M. W., D. J. Filman, E. A. Stura, S. Guillot, F. Delpeyroux, R. Crainic, and J. M. Hogle.** 1995. Structure of the complex between the Fab fragment of a neutralizing antibody for type 1 poliovirus and its viral epitope. Nat. Struct. Biol. **2:**232–243.
54. **Yang, X., I. Lipchina, M. Lifson, L. Wang, and J. Sodroski.** 2007. Antibody binding in proximity to the receptor/glycoprotein complex leads to a basal level of virus neutralization. J. Virol. **81:**8809–8813.
55. **Yang, Z. Y., Y. Huang, L. Ganesh, K. Leung, W. P. Kong, O. Schwartz, K. Subbarao, and G. J. Nabel.** 2004. pH-dependent entry of severe acute respiratory syndrome coronavirus is mediated by the spike glycoprotein and enhanced by dendritic cell transfer through DC-SIGN. J. Virol. **78:**5642–5650.
56. **Yang, Z. Y., H. C. Werner, W. P. Kong, K. Leung, E. Traggiai, A. Lanzavecchia, and G. J. Nabel.** 2005. Evasion of antibody neutralization in emerging severe acute respiratory syndrome coronaviruses. Proc. Natl. Acad. Sci. USA **102:**797–801.
57. **Zhu, Z., S. Chakraborti, Y. He, A. Roberts, T. Sheahan, X. Xiao, L. E. Hensley, P. Prabakaran, B. Rockx, I. A. Sidorov, D. Corti, L. Vogel, Y. Feng, J. O. Kim, L. F. Wang, R. Baric, A. Lanzavecchia, K. M. Curtis, G. J. Nabel, K. Subbarao, S. Jiang, and D. S. Dimitrov.** 2007. Potent cross-reactive neutralization of SARS coronavirus isolates by human monoclonal antibodies. Proc. Natl. Acad. Sci. USA **104:**12123–12128.